LONG-TERM (2012-2022) SPATIOTEMPORAL MODIS-DERIVED AEROSOL OPTICAL DEPTH ANALYSIS OF IĞDIR CITY, TÜRKİYE

DOI: https://doi.org/10.18509/GBP23225s
UDC: 528.88.06:[502.3:504.5"2012/22"(560)

Aliihsan Sekertekin[1]
Fatemeh Ghasempour[2]
Senol Hakan Kutoglu[2]
[1]Department of Architecture and Town Planning, Vocational School of Higher Education for Technical Sciences, Igdir University, **Türkiye**
[2]Department of Geomatics Engineering, Zonguldak Bulent Ecevit University, Zonguldak, **Türkiye**

ABSTRACT

Remote sensing (RS) technologies provide valuable information about air quality assessment in various scales and time intervals, which enables understanding the effects and trends of anthropogenic activities. Atmospheric aerosols are generally monitored using satellite-based Aerosol Optical Depth (AOD) data. Moderate Resolution Imaging Spectroradiometer (MODIS) aboard the Aqua and Terra satellites is one of the primary sources that makes it possible to obtain daily AOD observations. In this study, we aim to evaluate long-term (2012-2022) spatiotemporal MODIS-derived AOD data over Iğdır Province of Türkiye with wind properties. Concerning air pollution, Iğdır is one of the most polluted cities not only in Türkiye but also in Europe. Thus, continuous and long-term monitoring of air quality in Iğdır city is vital for the environmental sustainability and public health. For spatiotemporal analysis, seasonal AOD images were extracted for each year, from 2012 to 2022, and then mean of them were calculated to obtain long-term mean seasonal AOD images. Overall, the mean seasonal AOD values varied almost between 0 and 0.4. The results showed that in general the northern part of the study area has higher AOD values than the southern part, except for the mean of the spring seasons. On the other hand, the wind pattern, in mean seasonal summer, is almost opposite to the other mean seasonal wind directions. This research presents preliminary results, thus to reveal the main source of the aerosols, extensive multisiciplinary study should be conducted in the study area.

Keywords: Air Quality, Air Pollution, Wind Direction, MODIS AOD, Iğdır, Türkiye

INTRODUCTION

Aerosols are tiny particles, which are suspended in the atmosphere with aerodynamic diameters between 0.001-100 μm, and they play a significant role in human health [1, 2], earth-atmosphere radiation balance [3, 4], aerosol-cloud interaction [5], climate change obtained by diminishing or reinforcing the warming at regional and global scales [6, 7]. In order to monitor Aerosol Optical Depth (AOD), there are two different data sets, including ground-level monitoring/station data and satellite-based observations [8-11]. Compared to the ground-based observations, satellite-derived AOD measurements enable long-term AOD monitoring at a regional or global scale [12]. In particular, the Multi-Angle Implementation of Atmospheric Correction (MAIAC) AOD product extracted from Terra and Aqua satellites at high spatial and temporal resolution (1 km, daily) has

provided a distinctive opportunity to investigate the micro-scale AOD changes over time and space [13, 14]. It is worth mentioning that satellite-derived AOD data usually endure missing data due to the bright surfaces or the surfaces covered by cloud/snow [12, 15]. To compensate the missing data gaps in the satellite-derived AOD, various methods have been offered with numerous spatial and temporal coverages [16, 17]. In this study, the missing data issue was not handled since long-term mean images eliminated the cloud problem, except for the winter season. This paper aims to investigate the spatial and temporal analysis of long-term (from 2012 to 2022) MODIS-derived AOD over Iğdır province, Türkiye, with wind direction vectors extracted from monthly aggregated ERA5.

STUDY AREA

Figure 1 illustrates the study area considered in this research. Iğdır province, with 3 districts and 163 villages (http://www.igdir.gov.tr/ilcelerimiz/), is located in the Eastern Anatolia Region of Türkiye and along the borders with the countries of Armenia, Iran, and Azerbaijan. It occupies an area of 3,539.00 km^2 and a total population of 203,594.00. Its average altitude is about 850 m from the mean sea level and there is a continental semi-arid climate with hot-dry summers and cold-snowy winters. It is also one of the driest cities in Türkiye with an average precipitation of about 261 mm per year. Air pollution is intensely experienced in the province because of the geographical location, topographic structure, meteorological conditions, microclimate features and a high level of pollution due to the inversion event.

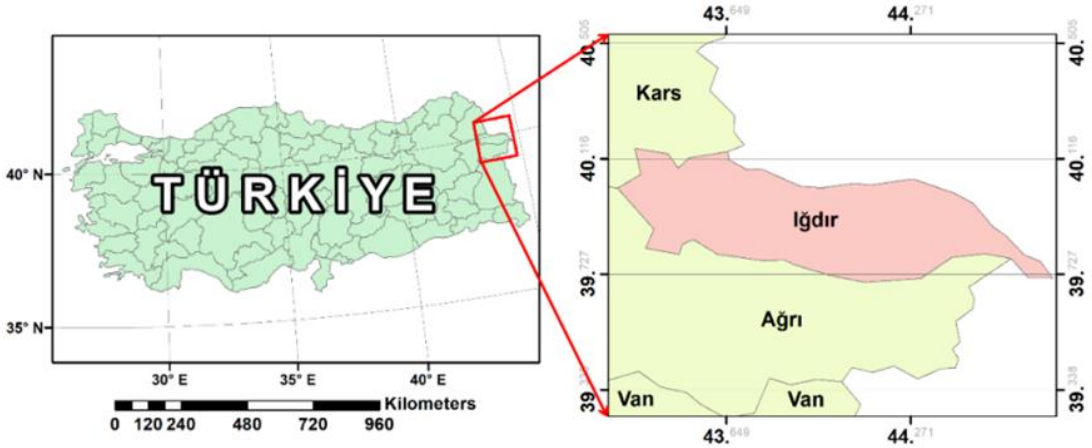

Figure 1. The location map of the study area

RESEARCH DATASET

In this study, we utilized two different sources of the dataset, MODIS-derived AOD dataset at 470nm and ERA5-derived wind components between 2012 and 2022. To trace atmospheric aerosols, we collected the daily AOD images of MODIS (MODIS/006/MCD19A2_GRANULES), which are freely accessible in the Google Earth Engine (GEE) data catalog. This product is provided by the Land Processes Distributed Active Archive Center (LP DAAC) within the NASA Earth Observing System Data and Information System (EOSDIS) located at the USGS Earth Resources observation and science (EROS) center [18]. ERA5 is a global climate/weather reanalysis dataset launched by the European Center for Medium-range Weather Forecasts (ECMWF) under the Copernicus Climate Change Service [19]. To prepare a reanalysis dataset, a

combination of model data with a wide range of sensor- and ground-based observations, including different meteorological parameters, are utilized based on the laws of physics. We employed the monthly aggregate of ECMWF ERA5 land data (ECMWF/ERA5_LAND/MONTHLY_AGGR) in this study, and we investigated the visualized relationship between satellite-derived AOD and ERA5-based zonal and meridional wind at the spatial resolution of 0.25◦ × 0.25◦.

METHODOLOGY

To investigate the long-term spatiotemporal changes of AOD over Iğdır province, the methodological steps were performed in GEE cloud platform. Figure 2 illustrates the methodology on a work-flow scheme. The main steps in the methodology are divided into three sections, namely, pre-processing, processing, and exports, referring to grey, orange, and green colors, respectively.

The grey-colored pre-processing step contains the following sub-steps:

MODIS-derived AOD

- Filter image collection by date: the prime step is the introducing of the interested period (2012-2022) as an input parameter.
- Select the interested band: AOD data collection is derived from two different wavelengths including blue and green bands. We opted blue band AOD at a wavelength of 470nm.
- Multiply all images to a scale factor: according to the AOD image collection in Earth Engine Data Catalog, it is essential to apply a scale factor value of 0.001 to all images.
- Clip all image collection over the region of interest: to investigate the variations over the study area.

ERA5-derived meteorological parameter

- Filter date on the dataset between 2012 and 2022: this step is applied to collect the data for the corresponding time interval.
- Select interested bands as u- and v- components of wind at the height of 10m from the ground surface: ERA-5 wind data collection are derived into two components as two different direction of Cartesian coordinate system. U-component is in the west-ward direction called zonal component while V-component is in the south-ward direction called meridian component. To calculate the true wind direction and wind speed, we used these components.
- Clip all image collection over Iğdır province.
- Calculate the wind speed values and wind direction vectors based on equations (1) and (2)

$$T = \left(T_u^2 + T_v^2\right)^{0.5} \quad (1)$$

$$T_\theta = 270^o - \arctan(T_v/T_u) \quad (2)$$

Where T, T_θ, T_u, and T_v are wind speed value, wind direction, and zonal and meridional components, respectively.

The processing step with orange color includes functions for extracting seasonal average images including the period from 2012 to 2022. Therefore, we extracted the four image sets as the four seasons for each year.

The green-colored results extracted from the processing step demonstrated two different formats including charts and visualized maps. It is worth noting that visualized maps are comprised the 44 seasonal maps and 4 long-term mean seasonal maps.

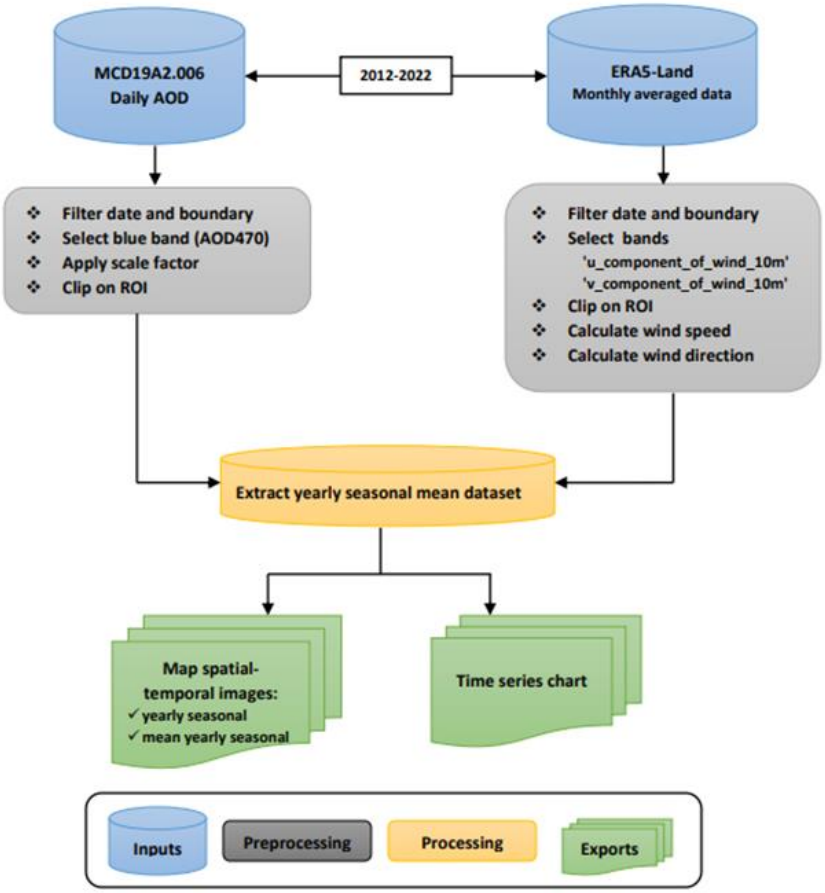

Figure 2. The work-flow scheme used in this study

RESULTS

As stated in the methodology, from 2012 to 2022, seasonal AOD images were extracted for each year. Therefore, we had four AOD images representing spring, summer, fall, and winter for each year. After extracting these seasonal AOD images, mean of them were calculated to obtain long-term mean seasonal AOD images for the study area. Overall, the mean seasonal AOD values varied almost between 0 and 0.4. Figure 3 represents long-term (11-year) mean spring AOD image with seasonal mean wind properties on it. The wind speed is associated with the length of the black bar, and the red circle shows the wind direction. Concerning the long-term mean spring AOD image (Figure 3), it is clear that dense AOD distribution is observed at the Southwest of the study area, and also the Northeast parts have average AOD pattern based on the legend. The wind direction is mainly from south to north and the wind speed is higher at the west side from the middle of the study area. Figure 4 illustrates the long-term (11-year) mean summer AOD image. This mean summer AOD image reveals that most of the study area has high aerosol concentration except for a small area at the southern and western parts of the study area. Considering the wind properties in Figure 4, the wind pattern is almost opposite to the springtime in Figure 3. Figure 5 and Figure 6 show the long-term (11-year) mean fall and winter AOD images, respectively. The wind pattern in these images demonstrates similar

trend as in springtime. Additionally, the severity of the wind speed in the long-term mean winter AOD image is the highest among all long-term mean images. In Figure 5, it is clear that the distribution of the aerosol concentration is not very high in long-term mean fall image. On the other hand, in the long-term mean winter image (Figure 6), the AOD values are higher at the Northern part compared to the Southern part. Besides, the missing data are observed at the Southern part of the image in Figure 6 due to long-term seasonal cloud coverage. In general, the primary sources of aerosols are biomass burning smoke and urban/industrial emissions, while the secondary sources are gaseous aerosol precursors, dust and sea salt. In this study, the main source of the aerosol distribution is most probably related to the desertification around the study area. Due to the desertification, particulate matters are transported via the wind. In order to prove the main sources of aerosols in the study area, multidisciplinary and extensive research is required.

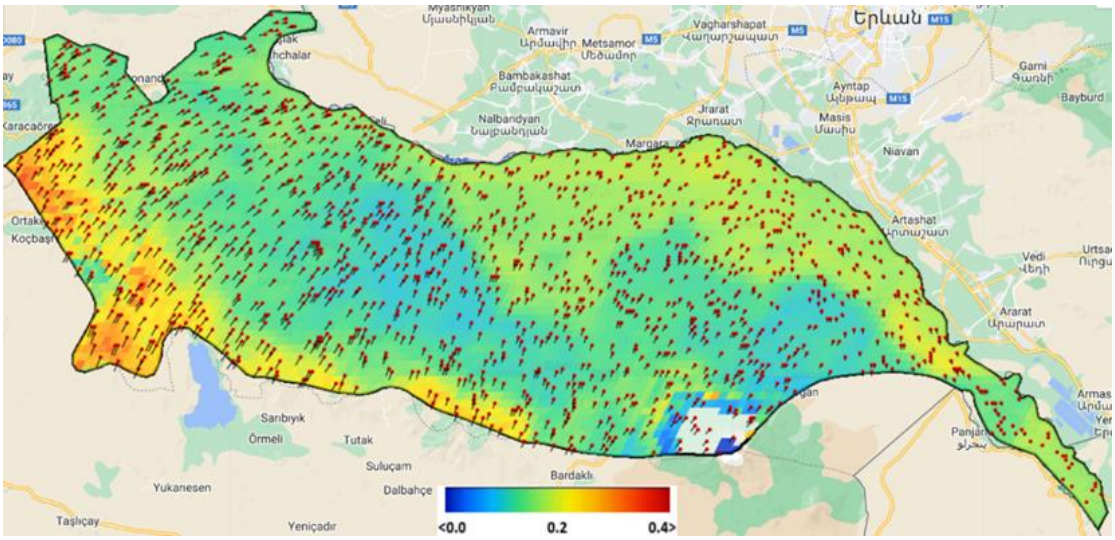

Figure 3. Long-term (11-year) mean spring AOD image with seasonal mean wind properties

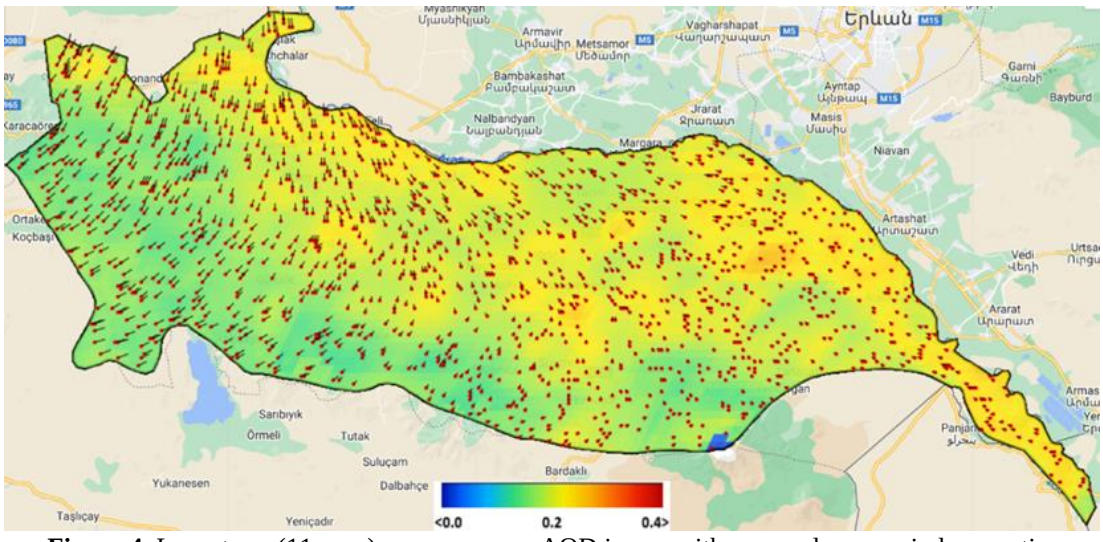

Figure 4. Long-term (11-year) mean summer AOD image with seasonal mean wind properties

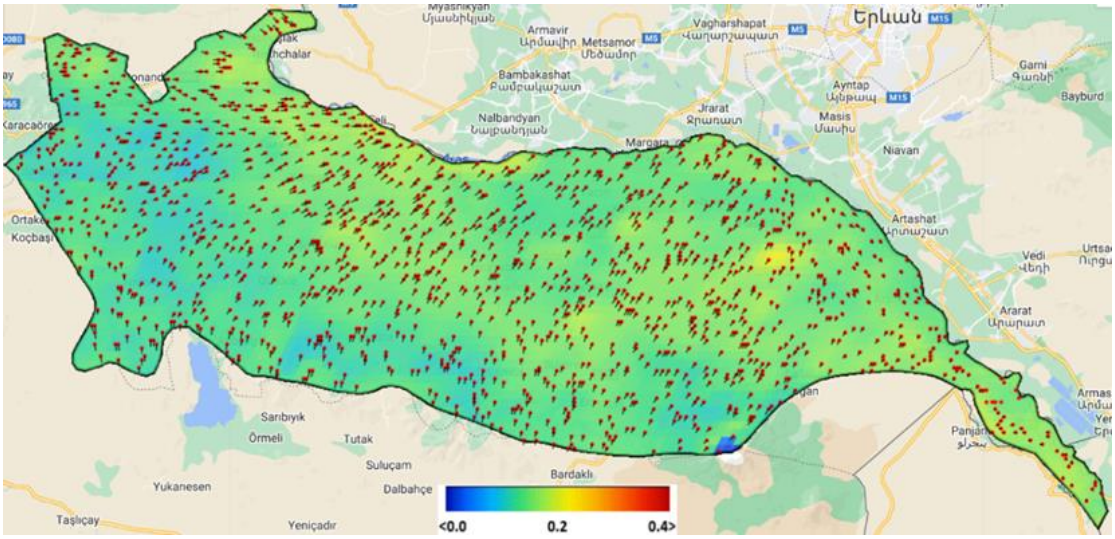

Figure 5. Long-term (11-year) mean fall AOD image with seasonal mean wind properties.

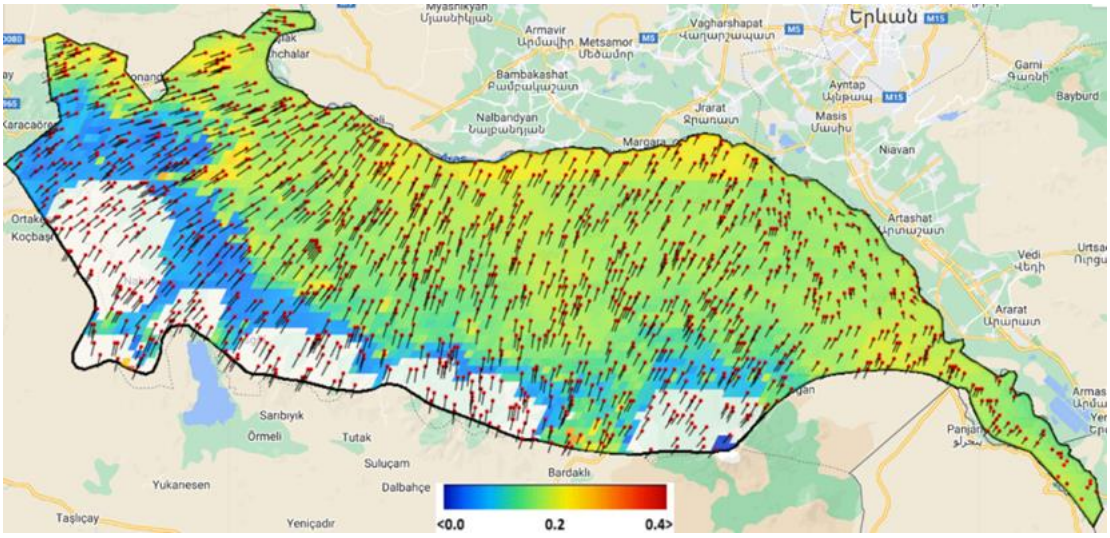

Figure 6. Long-term (11-year) mean winter AOD image with seasonal mean wind properties.

CONCLUSIONS

In this preliminary research, long-term (from 2012 to 2022) seasonal MODIS-derived AOD was investigated over Iğdır province, Türkiye, together with seasonal mean wind properties. The methodological steps were performed in the GEE cloud platform to extract seasonal mean AOD and wind maps. The results showed that in general the northern part of the study area has higher AOD values than the southern part, except for the mean of the spring seasons. On the other hand, the wind pattern, in mean seasonal summer, is almost opposite to the other mean seasonal wind directions. The study area is an important agricultural region; however, desertification issue is observed around its surrounding. Thus, this issue is thought as the main source of the aerosols in this area because of the particulate matters that are transported via the wind. In order to prove this argument, extensive studies should be conducted with other disciplines that will reveal the source of the aerosol in the study area.

REFERENCES

[1] Q. Wang, C. Liu, S. Sun, G. Yang, J. Luo, N. Wang, B. Chen, L. Wang, Enhance antibiotic resistance and human health risks in aerosols during the COVID-19 pandemic, Science of The Total Environment 871 (2023) 162035.

[2] S. Uddin, S.W. Fowler, N. Habibi, S. Sajid, S. Dupont, M. Behbehani, A preliminary assessment of size-fractionated microplastics in indoor aerosol—Kuwait's baseline, Toxics 10(2) (2022) 71.

[3] B. De Rosa, L. Mona, S. Lolli, A. Amodeo, M. Mytilinaios, Columnar heating rate and radiative effects of dust aerosols using 20 years of lidar observations, Copernicus Meetings, 2023.

[4] Z. Mushtaq, M. Sharma, P. Bangotra, A.S. Gautam, S. Gautam, Atmospheric aerosols: some highlights and highlighters, past to recent years, Aerosol Science and Engineering 6(2) (2022) 135-145.

[5] J.M. Haywood, S.J. Abel, P.A. Barrett, N. Bellouin, A. Blyth, K.N. Bower, M. Brooks, K. Carslaw, H. Che, H. Coe, The CLoud–Aerosol–Radiation interaction and forcing: Year 2017 (CLARIFY-2017) measurement campaign, Atmospheric Chemistry and Physics 21(2) (2021) 1049-1084.

[6] P. Wang, Q. Tang, Y. Zhu, Y. He, Q. Yu, T. Liang, K. Zheng, Spatial-Temporal Variation of AOD Based on MAIAC AOD in East Asia from 2011 to 2020, Atmosphere 13(12) (2022) 1983.

[7] J. Schmale, P. Zieger, A.M. Ekman, Aerosols in current and future Arctic climate, Nature Climate Change 11(2) (2021) 95-105.

[8] D. Kong, H. He, J. Zhao, J. Ma, W. Gong, Aerosol Property Analysis Based on Ground-Based Lidar in Sansha, China, Atmosphere 13(9) (2022) 1511.

[9] X. Wu, J. Yuan, T. Wei, Y. Zhang, K. Wu, H. Xia, Variation of Aerosol Optical Depth Measured by Sun Photometer at a Rural Site near Beijing during the 2017–2019 Period, Remote Sensing 14(12) (2022) 2908.

[10] O. Pilahome, W. Ninssawan, Y. Jankondee, S. Janjai, W. Kumharn, Long-term variations and comparison of aerosol optical properties based on MODIS and ground-based data in Thailand, Atmospheric Environment 286 (2022) 119218.

[11] A.R.S. Abadi, N.H. Hamzeh, K. Shukurov, C. Opp, U.C. Dumka, Long-Term Investigation of Aerosols in the Urmia Lake Region in the Middle East by Ground-Based and Satellite Data in 2000–2021, Remote Sensing 14(15) (2022) 3827.

[12] Q. He, W. Wang, Y. Song, M. Zhang, B. Huang, Spatiotemporal high-resolution imputation modeling of aerosol optical depth for investigating its full-coverage variation in China from 2003 to 2020, Atmospheric Research 281 (2023) 106481.

[13] P. Wang, Q. Tang, Y. Zhu, K. Zheng, T. Liang, Q. Yu, Y. He, Validation and Analysis of MAIAC AOD Aerosol Products in East Asia from 2011 to 2020, Remote Sensing 14(22) (2022) 5735.

[14] M. Pedde, I. Kloog, A. Szpiro, M. Dorman, T.V. Larson, S.D. Adar, Estimating long-term PM10-2.5 concentrations in six US cities using satellite-based aerosol optical depth data, Atmospheric Environment 272 (2022) 118945.

[15] R. Gao, X. Rui, J. Tang, A Spatio-Temporal Weighted Filling Method for Missing AOD Values, Atmosphere 13(7) (2022) 1080.

[16] T. Zhang, Y. Zhou, K. Zhao, Z. Zhu, G.R. Asrar, X. Zhao, Gap-filling MODIS daily aerosol optical depth products by developing a spatiotemporal fitting algorithm, GIScience & Remote Sensing 59(1) (2022) 762-781.

[17] K. Bai, K. Li, M. Ma, K. Li, Z. Li, J. Guo, N.-B. Chang, Z. Tan, D. Han, LGHAP: the Long-term Gap-free High-resolution Air Pollutant concentration dataset, derived via tensor-flow-based multimodal data fusion, Earth System Science Data 14(2) (2022) 907-927.

[18] A. Lyapustin, Y. Wang, MCD19A2 MODIS/Terra+ aqua land aerosol optical depth daily L2G global 1km SIN grid V006 [data set], NASA EOSDIS land processes DAAC (2018).

[19] H. Hersbach, B. Bell, P. Berrisford, G. Biavati, A. Horányi, J. Muñoz Sabater, J. Nicolas, C. Peubey, R. Radu, I. Rozum, ERA5 hourly data on single levels from 1979 to present, Copernicus climate change service (c3s) climate data store (cds) 10(10.24381) (2018).